Hyperbranched Poly(silylenephenylenes) from Polycyclotrimerization of A_2-Type Diyne Monomers: Synthesis, Characterization, Structural Modeling, Thermal Stability, and Fluorescent Patterning

Jianzhao Liu,[†] Ronghua Zheng,[†] Youhong Tang,[‡] Matthias Häussler,[†] Jacky W. Y. Lam,[†] Anjun Qin,[†,§] Mingxin Ye,[†] Yuning Hong,[†] Ping Gao,[‡] and Ben Zhong Tang*[,†,§]

Department of Chemistry and Department of Chemical Engineering, The Hong Kong University of Science & Technology (HKUST), Clear Water Bay, Kowloon, Hong Kong, China, and Department of Polymer Science and Engineering, Zhejiang University, Hangzhou 310027, China

Received May 11, 2007; Revised Manuscript Received July 22, 2007

ABSTRACT: A group of hyperbranched poly(silylenephenylenes) (*hb*-PSPs) were synthesized in high yields (up to 100%) by $TaBr_5$-catalyzed polycyclotrimerization of A_2-type monomers of silylenediynes [HC≡C−C_6H_4−Si(C_nH_{2n+1})$_2$−C_6H_4−C≡CH, n = 2, 4, 6]. The *hb*-PSPs are completely soluble in common organic solvents such as chloroform, toluene, and THF. Spectroscopic and modeling studies confirmed that the polymers had formed via a [2 + 2 + 2] cyclotrimerization mechanism. Analysis of the triple-bond conversion processes led to the establishment of a relationship between the degree of branching and the fraction of dendritic unit. Computational simulation shed light on the real topological structures of the *hb*-PSPs. The polymers lost little weights when heated up to 480 °C and carbonize in high yields (up to 71%) after pyrolysis at 800 °C. The *hb*-PSPs possess a unique $\sigma-\pi$ conjugated electronic structure and emit strong violet-blue light upon photoexcitation. The triple bonds on the peripheries allowed the thin films of the polymers to be readily photo-cross-linked, generating fluorescent photoimages in high resolutions.

Introduction

With a globular architecture and numerous end groups on the peripheries, hyperbranched polymers have attracted much attention among polymer scientists.[1−10] In comparison to their perfect dendritic congeners, hyperbranched polymers are easer to prepare, with their syntheses accomplishable by simple, single-step procedures. Organosilicon hyperbranched polymers are organic−inorganic hybrids and are promising precursors to functional ceramics, degradable templates, and high-temperature elastomers.[11−16] The silicon-containing polymers have usually been prepared by the hydrosilylation polymerizations of AB_n monomers, where A and B denote functional groups of silane (Si−H) and olefin (−CH═CH_2) [or acetylene (−C≡CH)], respectively, with $n \geq 2$.[17−19]

Our research groups have worked on the synthesis of hyperbranched conjugated polymers by diyne polycyclotrimerizations.[20−25] Through elaborate efforts, we have succeeded in the preparation of a wide variety of functional hyperbranched polyphenylenes by homopolycyclotrimerizations of aryldiynes and their copolycyclotrimerizations with aromatic or aliphatic monoynes.[26−32] The polymers have been found to exhibit an array of unique properties, such as high thermal stability (up to ∼500 °C), ready photocurability, efficient light emission (quantum yield up to 98%), large optical nonlinearity, and low optical dispersion (down to 0.009).[25]

The polycyclotrimerization of aromatic diyne is particularly intriguing because it uses only a single A_2-type monomer. The commonly taken synthetic approaches to hyperbranched polymers have been polycondensations of AB_2- and (A_2 + B_3)-type monomers (Scheme 1). The former approach, however, suffers from the synthetic difficulty in the monomer preparation and the self-oligomerization during the monomer storage due to the coexistence of two mutually reactive functional groups (A and B) in one monomer structure, while the latter approach requires stoichiometric balance of the two monomers (A_2 and B_3) in order to get polymers with high molecular weights (MWs) and degrees of branching (DBs).

In contrast, the A_2-type diyne monomers are stable at room temperature in the absence of a catalytic species and their transition metal-catalyzed polycyclotrimerizations are unimolecular events. In other words, there are no complications of self-oligomerization and requirements of stoichiometric balance in the diyne systems, whose polymerizations can thus potentially produce hyperbranched polymers with very high MWs and DBs. However, the direct knitting of the rigid, planar aromatic rings in the polymer structure, together with their facile $\pi-\pi$ stacking, often leads to poor solubility of the polymers, which significantly limits the scope of their technological applications.

To overcome this limitation and to enrich the research area of hyperbranched organosilicon polymers, in this work, we prepared a group of new silylenediyne (SDY) monomers (Scheme 2). A nonplanar silyl spacer is used to separate two phenylacetylene units, in the hope that the spacer will reduce the overall rigidity and symmetry of the structure of the resultant polymer, hence hampering the $\pi-\pi$ stacking of its branch units. The monomers were effectively polycyclotrimerized by a single-component catalyst of $TaBr_5$ to give hyperbranched poly(silylenephenylenes) (*hb*-PSPs) in high yields (Scheme 3). In this paper, we report the polymerization behaviors of the SDY monomers and the detailed studies on the structures and properties of the resultant polymers.

* Corresponding author. Telephone: +852-2358-7375. Fax: +852-2358-1594. E-mail: tangbenz@ust.hk.
† Department of Chemistry, HKUST.
‡ Department of Chemical Engineering, HKUST.
§ Zhejiang University.

10.1021/ma071062d CCC: $37.00
Published on Web 09/21/2007

Scheme 1

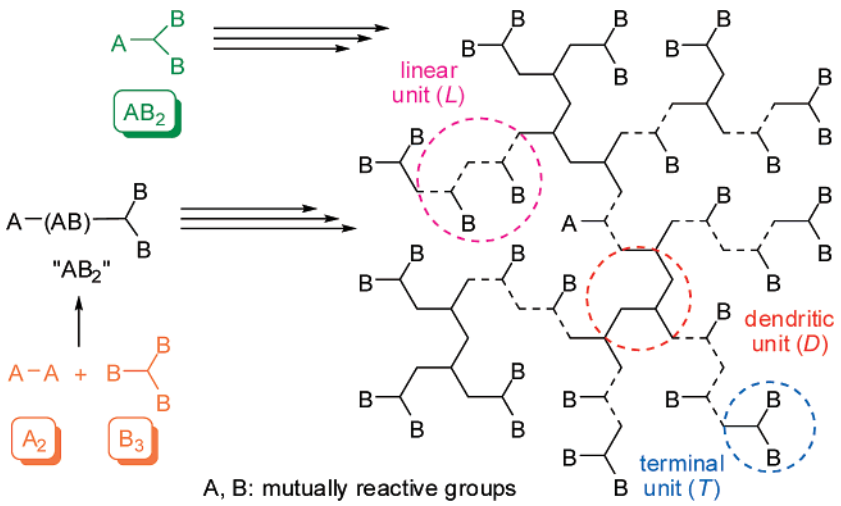

Scheme 2

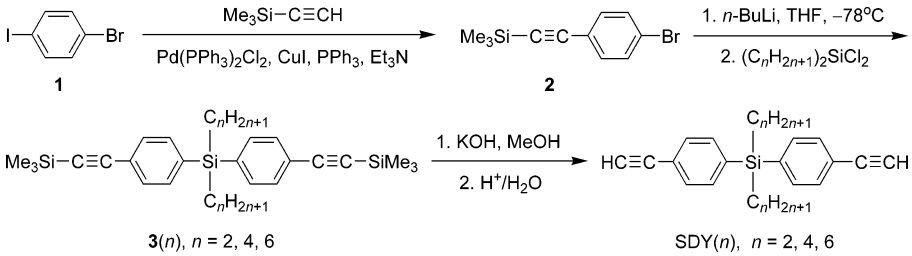

Results and Discussion

Monomer Synthesis. The organosilicon monomers SDY(*n*) carrying alkyl groups of various chain lengths ($n = 2, 4, 6$) are readily accessible by a three-step synthetic protocol (cf. Scheme 2). Palladium-catalyzed Sonogashira coupling of 1-bromo-4-iodobenzene (**1**) with trimethylsilylacetylene furnishes monoacetylenic intermediate **2** in a high yield (97%). Lithiation of **2** with *n*-butyllithium followed by silylation with dichlorosilanes yields compounds **3**(*n*). Finally, base-catalyzed desilylation of **3**(*n*) in methanolic KOH solution completes the monomer synthesis. All the diyne monomers were thoroughly purified and fully characterized by standard spectroscopic methods, from which satisfactory analysis data corresponding to their expected molecular structures were obtained (see Experimental Section for details).

Polymerization Behaviors. After obtaining the SDY monomers, we systematically investigated their polymerization behaviors, in an effort to optimize the reaction conditions. We first examined the effect of solvent on the diyne polycyclotrimerizations. Table 1 lists the results of polymerizations of bis(4-ethynylphenyl)diethylsilane [SDY(2)] catalyzed by $TaBr_5$. No polymers are obtained in dioxane and tetrahydrofuran (THF), and only trace amounts of polymeric products are formed in dichloromethane (DCM) and hexane (Table 1, nos. 1−4). Delightfully, however, polymers with high molecular weights ($M_w \sim 14000$) are obtained in a high yield (~90%) when the reaction is conducted in toluene. Moreover, the polymer is completely soluble in common organic solvents such as toluene, chloroform, and THF.

We followed the time courses of the SDY polycyclotrimerizations. The polymerization of SDY(2) steadily proceeds: both the yield and M_w increase with an increase in the reaction time (Table 2, nos. 1−7). The PDI of the polymer also increases with time, but its highest value is 2.6, which is considered to be "low" for a hyperbranched polymer, noting that polymers with PDIs up to ~35 have been formed in our previous studies.[28] The length of the alkyl chain (*n*) adversely affects the polymerizability of the monomer. Under the similar reaction conditions, SDY(2) can be polymerized in high yields in 1−6 h, while polymers are obtained in trace amounts or low yields from the reactions of its congeners with longer alkyl chains [i.e., SDY(4) and SDY(6)]. These monomers may experience more serious steric effects and their triple bonds may have lower chances to collide to form benzene rings. Longer reaction times are thus needed to obtain appreciable amounts of polymers with reasonable molecular weights from their polymerization reactions.

Tetraphenyltin has often been used as a cocatalyst in the diyne polycyclotrimerization.[25] Its addition into the reaction mixtures has, however, little effects on the $TaBr_5$-catalyzed polymerizations (Table 3). In two occasions, even an adverse effect is observed (cf., Table 3, nos. 1 and 2, and nos. 3 and 4). To prepare the binary catalyst solution, stoichiometric amounts of $TaBr_5$ and Ph_4Sn need to be admixed in a proper solvent and aged for an adequate period at a desired temperature. In comparison to the binary mixture, the single-component catalyst is preferable and is particularly welcomed by industrial process engineers because of its lower cost, easier handling, and simpler operation. The single-component catalyst system is thus used in all the subsequent experiments in this study.

The effect of temperature on the polycyclotrimerizations is summarized in Table 4. With an increase in the temperature, the reaction rate and the polymer yield are increased. Raising the temperature thus shortens the polymerization time. For example, the polymerization of SDY(6) at room temperature for 8 h gives an *hb*-PSP(6) with an M_w of ~5000 in ~24% yield, while at 80 °C only 6 min are needed to produce a polymeric product with an M_w of ~17000 in ~85% yield (cf., Table 4, nos. 8 and 10). The polymerization at high temperatures, however, becomes less controlled, easily resulting in the formation of insoluble gels. Although requiring somewhat longer

Scheme 3

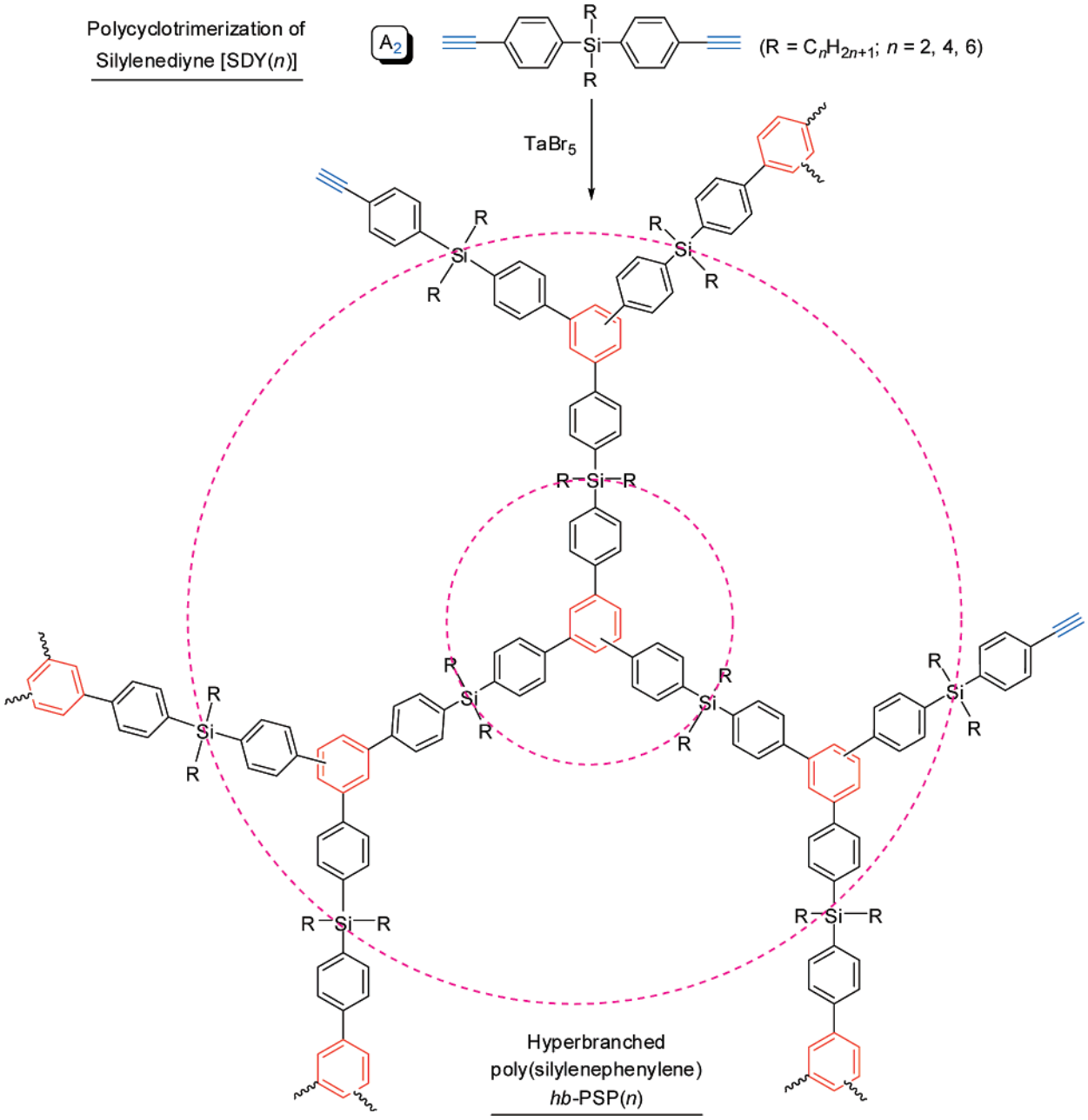

Table 1. Effect of Solvent on the Polymerization of Bis(4-ethynylphenyl)diethylsilane [SDY(2)][a]

no.	solvent	yield (%)	S[b]	M_w[c]	M_w/M_n[c]
1	dioxane	0			
2	THF	0			
3	DCM	trace	√		
4	hexane	trace	√		
5	toluene	90.2	√	13800	2.6

[a] Polymerization reaction carried out at room temperature under nitrogen for 6 h using $TaBr_5$ as catalyst; [cat.] = 5 mM, $[M]_0$ = 0.1 M. [b] Solubility (S) tested in common organic solvents such as THF, toluene, DCM, and chloroform; √ = completely soluble. [c] Estimated by gel-permeation chromatography (GPC) in THF on the basis of a polystyrene calibration; M_w = weight-average molecular weight; M_w/M_n = polydispersity index (PDI); M_n = number-average molecular weight.

times, most of the polymerization reactions in this work are still conducted at room temperature, because it can afford soluble polymers with high enough molecular weights in reasonable yields.

We carried out the polymerization reactions at different catalyst and monomer concentrations (Tables 5 and 6). The effect of the catalyst concentration was investigated at different sets of reaction times. Comparing the polymerization results obtained at catalyst concentrations of 5 and 10 mM at the same reaction times, it is found that polymers with higher molecular weights are always obtained in higher yields at the higher catalyst concentration. For example, at 5 mM of [cat.], an *hb*-PSP(4) with an M_w of 2600 is obtained in ~12% in 8 h; increasing the [cat.] to 10 mM dramatically boosts the M_w and yield to 13200 and ~86%, respectively (cf., Table 5, nos. 3 and 4). Likewise, the monomer concentration also affects the polycyclotrimerization. The polymerization performed at higher monomer concentrations gives higher molecular weight polymers in shorter times. For example, when 0.1 M of $[M]_0$ is used, an *hb*-PSP(4) with an M_w of 13600 is obtained in 100% in 8 h, while at 0.05 M of $[M]_0$, the M_w and yield are 10500 and ~85%, respectively (cf., Table 6, nos. 5 and 6).

Table 2. Time Courses of the Polymerizations of Silylenediynes [SDY(*n*)][a]

no.	monomer	time (h)	yield (%)	S[b]	M_w[c]	M_w/M_n[c]
1	SDY(2)	0.5	41.6	√	3100	1.2
2		1	75.2	√	3500	1.3
3		2	80.9	√	6200	1.5
4		4	100	√	7100	1.8
5		6	90.2	√	13800	2.6
6		8	84.4	√	11900	2.6
7		12	93.6	Δ		
8	SDY(4)	0.5	trace	√		
9		2	trace	√		
10		4	4.3	√	1500	1.9
11		6	5.8	√	3400	1.4
12		24	81.3	√	9300	1.8
13	SDY(6)	0.5	trace	√		
14		6	trace	√		
15		24	100	√	13500	2.1

[a] Polymerization reactions carried out in toluene at room temperature under nitrogen using $TaBr_5$ as catalyst; [cat.] = 5 mM, $[M]_0$ = 0.1 M. [b] Solubility tested in common organic solvents; √ = completely soluble, Δ = partially soluble. [c] Estimated by GPC in THF on the basis of a polystyrene calibration.

Table 3. Effect of Cocatalyst on the Polymerizations of Silylenediynes [SDY(*n*)][a]

no.	catalyst	monomer	time (h)	yield (%)	S[b]	M_w[c]	M_w/M_n[c]
1	$TaBr_5$	SDY(4)	8	11.6	√	2600	1.2
2	$TaBr_5-Ph_4Sn$		8	8.7	√	2600	1.2
3	$TaBr_5$		24	81.3	√	9300	1.8
4	$TaBr_5-Ph_4Sn$		24	76.9	√	9000	1.8
5	$TaBr_5$	SDY(6)	8	23.7	√	4700	1.5
6	$TaBr_5-Ph_4Sn$		8	25.6	√	5100	1.5
7	$TaBr_5$		24	100	√	13500	2.1
8	$TaBr_5-Ph_4Sn$		24	100	√	14600	1.9

[a] Polymerization reactions carried out in toluene at room temperature under nitrogen; $[M]_0$ = 0.1 M, [cat.] = 5 mM. [b] Solubility tested in common organic solvents. [c] Estimated by GPC in THF on the basis of a polystyrene calibration.

Table 4. Effect of Temperature on the Polymerizations of Silylenediynes [SDY(*n*)][a]

no.	monomer	temp (°C)	time (h)	yield (%)	S[b]	M_w[c]	M_w/M_n[c]
1	SDY(2)	rt[d]	6	90.2	√	13800	2.6
2		40	6	100	Δ		
3		60	2	100	×		
4		80	1	100	×		
5	SDY(4)	rt	8	11.6	√	2600	1.2
6		80	2	100	Δ		
7		80	1	85.5	√	4400	1.3
8	SDY(6)	rt	8	23.7	√	4700	1.5
9		80	0.3	100	×		
10		80	0.1	84.9	√	17300	1.9

[a] Polymerization reaction carried out in toluene under nitrogen using $TaBr_5$ as catalyst; [cat.] = 5 mM, $[M]_0$ = 0.1 M. [b] Solubility tested in common organic solvents: √ = completely soluble, Δ = partially soluble, × = insoluble (gel). [c] Estimated by GPC in THF on the basis of a polystyrene calibration. [d] rt = room temperature.

To summarize, we have carefully studied the effects of solvent, reaction time, cocatalyst, temperature, and catalyst and monomer concentrations on the polycyclotrimerizations of SDY(*n*), which enabled us to optimize the reaction parameters for the preparation of soluble *hb*-PSPs with high molecular weights in high yields. The sp^3-hybridized, nonplanar silicon atoms impart large free volumes to the polymer structures, making the *hb*-PSPs highly soluble in common organic solvents.

Structural Characterization. The polymer products were fully characterized spectroscopically (see Experimental Section for detailed analysis data). The IR spectrum of *hb*-PSP(2) is given in Figure 1 as an example. The spectrum of its monomer [SDY(2)] is also shown in the same figure for the purpose of comparison. The strong absorption band observed at 3296 cm^{-1} in SDY(2) is associated with its ≡C−H stretching vibration. This band becomes weaker in the spectrum of its polymer, indicating that most of the triple bonds have been consumed by the polymerization reaction. The C≡C stretching vibration at 2108 cm^{-1} almost disappears after polymerization. Meanwhile, the absorption band of aromatic C═C skeleton vibration at 1594 cm^{-1} is intensified. All these spectral data prove that new benzene rings have been formed in the polymerization reaction.

Table 5. Effect of Catalyst Concentration on the Polymerizations of Silylenediynes [SDY(*n*)][a]

no.	monomer	[cat.] (mM)	time (h)	yield (%)	S[b]	M_w[c]	M_w/M_n[c]
1	SDY(4)	5	2	trace	√		
2		10	2	55.2	√	8800	1.8
3		5	8	11.6	√	2600	1.2
4		10	8	85.6	√	13200	2.3
5		5	24	81.3	√	9300	1.8
6		10	24	85.6	√	19300	2.7
7	SDY(6)	5	2	trace	√		
8		10	2	38.8	√	5400	1.5
9		5	8	23.7	√	4700	1.5
10		10	8	51.2	√	5000	1.4
11		5	24	100	√	13500	2.1
12		10	24	100	√	19700	2.5

[a] Polymerization reaction carried out in toluene at room temperature under nitrogen using $TaBr_5$ as catalyst; $[M]_0$ = 0.1 M. [b] Solubility tested in common organic solvents. [c] Estimated by GPC in THF on the basis of a polystyrene calibration.

Table 6. Effect of Monomer Concentration on the Polymerizations of Silylenediynes [SDY(*n*)][a]

no.	monomer	$[M]_o$ (M)	time (h)	yield (%)	S[b]	M_w[c]	M_w/M_n[c]
1	SDY(2)	0.05	6	100	√	13600	2.7
2		0.1	6	100	√	15400	2.6
3		0.15	6	100	√	19500	2.9
4		0.2	2	100	×		
5	SDY(4)	0.05	8	85.3	√	10500	2.0
6		0.1	8	100	√	13600	2.2
7		0.2	4	100	√	15300	2.2
8		0.3	4	93.7	×		

[a] Polymerization reaction carried out in toluene at room temperature under nitrogen using $TaBr_5$ as catalyst; [cat.] = 10 mM. [b] Solubility tested in common organic solvents. [c] Estimated by GPC in THF on the basis of a polystyrene calibration.

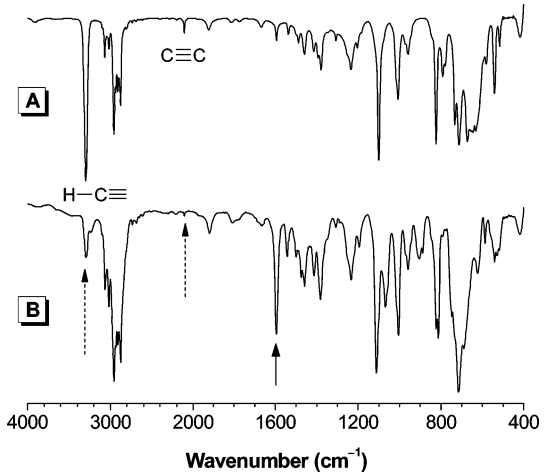

Figure 1. IR spectra of (A) monomer SDY(2) and (B) its polymer *hb*-PSP(2) (sample taken from Table 2, no. 6).

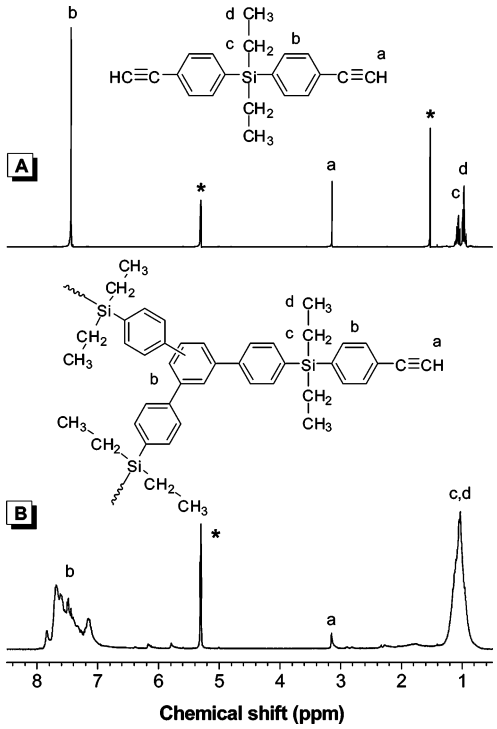

Figure 2. ^{1}H NMR spectra of DCM-d_2 solutions of (A) monomer SDY-(2) and (B) its polymer *hb*-PSP(2) (sample taken from Table 2, no. 6). The solvent peaks are marked with asterisks.

Similar results are obtained from NMR analyses. Figure 2 shows the ^{1}H NMR spectra of *hb*-PSP(2) and its monomer SDY-(2). The peak at δ 3.15 assigned to acetylene proton resonance of the monomer becomes weaker in the spectrum of its polymer, confirming that a large fraction of triple bonds have been consumed by the polymerization reaction. The unreacted triple bonds remain as end groups on the peripheries of the hyperbranched polymer. On the other hand, the resonance peaks in the aromatic region become broader and intensified after polymerization, substantiating that the acetylenic triple bonds of SDY(2) have been cyclotrimerized into benzene rings of *hb*-PSP(2). The ^{13}C NMR spectrum of the polymer shows weak resonance peaks of acetylenic carbon atoms at δ 84.0 and 78.2, with new peaks emerged in the aromatic carbon resonance region (Figure 3). These results again verify that many triple bonds have been transformed into benzene rings by the polycyclotrimerization reaction.

The above spectroscopic data confirm that new benzene rings have been formed in the polymerization reaction. The signals of the newly formed benzene rings in the polymers in the IR and NMR spectra are, however, overlapped with, and disturbed by, those of the "old" benzene rings originally existing in the monomers. To offer more experimental evidence and to gain more insights into the polymer structures, we designed and conducted two model reactions.

The first model reaction is the cyclotrimerization of phenylacetylene, a monoyne, catalyzed by $TaBr_5$ under the conditions same to those used in the polycyclotrimerizations of diynes SDY(*n*) (Scheme 4). No high molecular weight polymers are formed, which unambiguously rules out the possibility that the diynes have been polymerized into polyenes via a metathesis polymerization mechanism by $TaBr_5$.[33] The products of the model reaction are purified by silica gel column chromatography using hexane as eluent. ^{1}H NMR spectrum proves that the products are a mixture of 1,2,4- and 1,3,5-TPBs (Figure 4C). Recrystallization of the products gives pure isomers of 1,3,5-

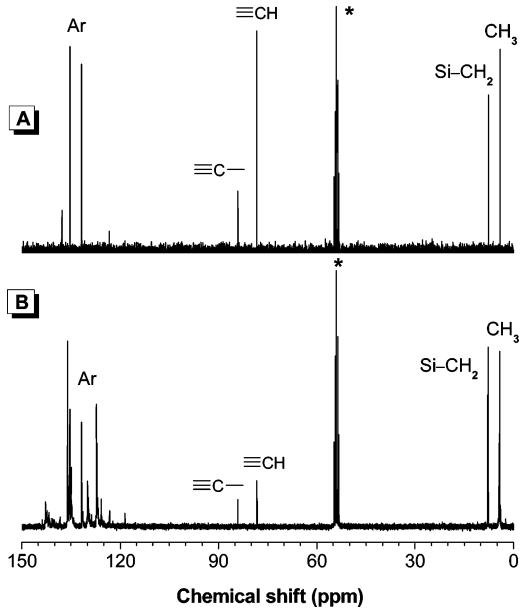

Figure 3. ^{13}C NMR spectra of DCM-d_2 solutions of (A) monomer SDY(2) and (B) its polymer *hb*-PSP(2) (sample taken from Table 2, no. 6). The solvent peaks are marked with asterisks.

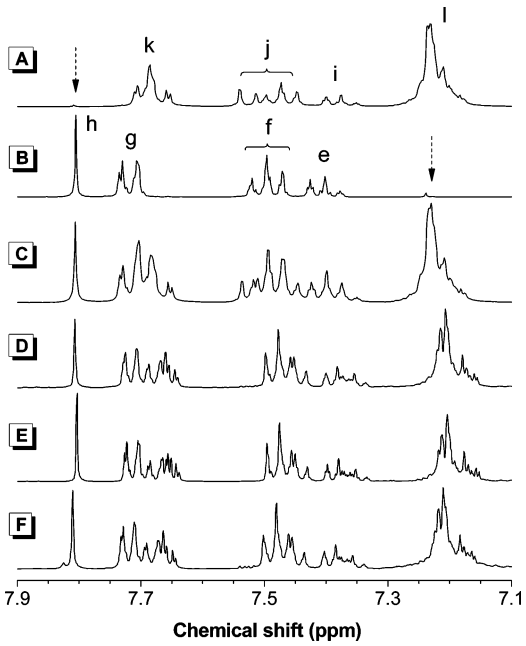

Figure 4. ^{1}H NMR spectra of (A) 1,2,4- and (B) 1,3,5-TPBs, (C) a mixture of 1,2,4- and 1,3,5-TPBs (products of the model reaction), and desilylated products of (D) *hb*-PSP(2) (sample taken from Table 6, no. 3), (E) *hb*-PSP(4) (Table 5, no. 6), and (F) *hb*-PSP(6) (Table 4, no. 10).

and 1,2,4-TPBs, whose ^{1}H NMR spectra are given in panels A and B of Figure 4. These results attest that the $TaBr_5$-catalyzed reaction has transformed three triple bonds into one benzene ring via a cyclotrimerization mechanism. From the ^{1}H NMR spectra of the mixture, the molar ratio of 1,3,5- to 1,2,4-TPB is calculated according to eq 1 to be 1.0:2.0.

$$\frac{N_{1,2,4}}{N_{1,3,5}} = \frac{A_l/10}{A_h/3} = \frac{3A_l}{10A_h} \tag{1}$$

where $N_{1,2,4}$ and $N_{1,3,5}$ are the numbers of 1,2,4- and 1,3,5-TPB rings and A_l and A_h are the integrated areas of resonance peaks l and h, respectively.

Scheme 4

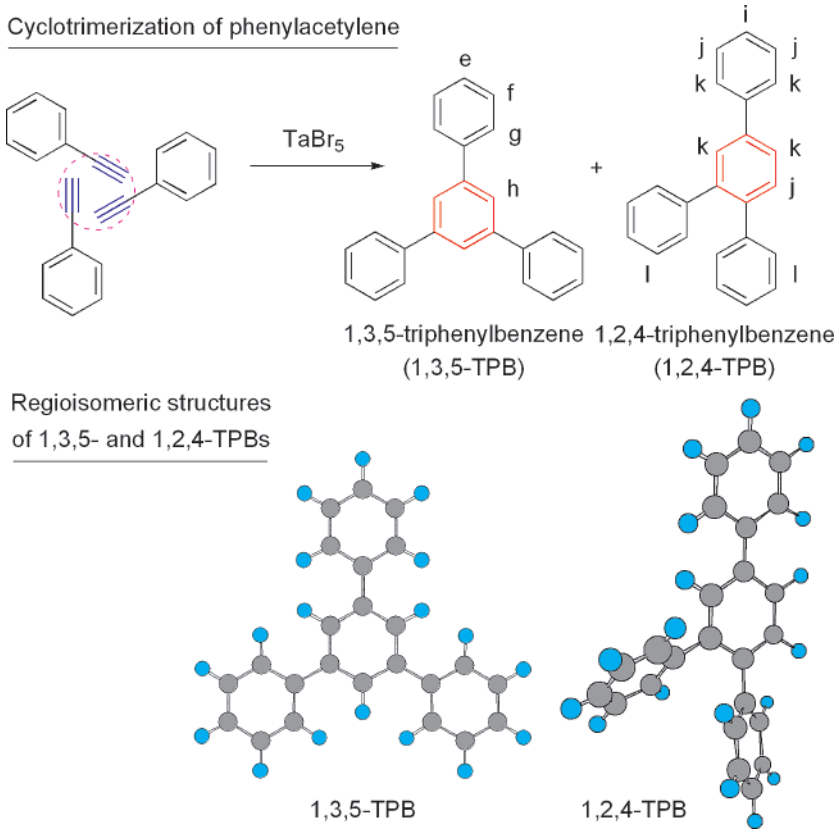

Scheme 5

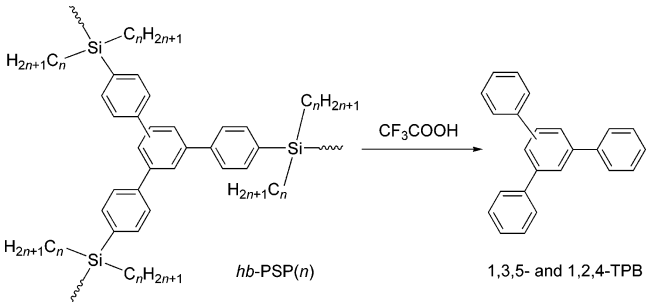

The second model reaction is the acid-catalyzed decomposition of *hb*-PSPs (Scheme 5). It is well-known that strong protonic acids such as CF_3COOH, $HClO_4$ and H_2SO_4 can promote the cleavage of Si−C bond.[34−36] When a mixture of *hb*-PSP(2) and CF_3COOH is refluxed in DCM for 96 h under nitrogen, the polymer decomposes to give TPBs, as confirmed by the IR, NMR, and MS analyses. The spectroscopic results further confirm that new benzene rings have been formed in the $TaBr_5$-catalyzed polymerization of SDY(2). An example of its ^1H NMR is given in Figure 4D. Calculations of the isomeric contents of 1,3,5- and 1,2,4-TPBs give a molar ratio of 1.0:2.0. The structures of *hb*-PSP(4) and *hb*-PSP(6) are analyzed under the same experimental conditions. The calculated molar ratios of 1,3,5- to 1,2,4-TPB for *hb*-PSP(4) and *hb*-PSP(6) are ∼1.0:1.7 and ∼1.0:1.9, respectively (panels E and F in Figure 4). The ratios derived from the decomposed products of *hb*-PSP(*n*) agree well with that obtained from the model reaction.

Theoretical Modeling. All the above results prove that the diynes have been cyclotrimerized to form new benzene rings with 1,2,4/1,3,5-isomeric structures. As confirmed by the spectroscopic analysis, the polymers contain unreacted triple bonds on their peripheries. To understand how the polymerization propagates, we tried to mathematically model the growth patterns of the polymer branches. On the basis of the experimental results, it is conjured that the monomers are transformed into various oligomer species by cyclotrimerization reactions, which further propagate to form the hyperbranched polymers (Scheme 6). Because of the high monomer concentration at the initial stage, three triple bonds from three different monomers can readily cyclotrimerize to form a benzene ring. The thus formed first generation (G_1) trimers continue to react with either monomers or other G_1 trimers. If one G_1 trimer reacts with two monomers, pentamer G_2-1 will be formed. In the same way, if cyclotrimerization occurs among two G_1 trimers and one monomer or three G_1 trimers, corresponding heptamer G_2-2 and nonamer G_2-3 will be furnished. We define this G_2-3 nonamer as the perfect second generation product and G_2-1 and G_2-2 as the imperfect ones. Further propagations will produce other oligomeric species with different sizes coexisting in the polymerization mixture.

Despite the different sizes of the propagating species, the growth modes can be divided into three categories, as shown as pathways A−C in Scheme 7. Pathway A is the normal growth mode, in which each of three oligomeric species contributes one triple bond to form a new benzene ring. The second pathway (B) is the cyclotrimerization between two oligomer species, in which one oligomer contributes two triple bonds and another contributes one triple bond to form a new benzene ring. This propagation mode leads to the formation of intramolecular loops inside a polymer. The third one (C) is a special intracyclotrimerization reaction, in which three triple bonds are from a same oligomer, resulting in the formation of a bicyclic structure. The polycyclotrimerizations should predominately propagate in mode A. The likelihoods for the polymerization reaction to propagate in modes B and C are much lower, due to the involved steric effects and mathematical probabilities.

Scheme 6

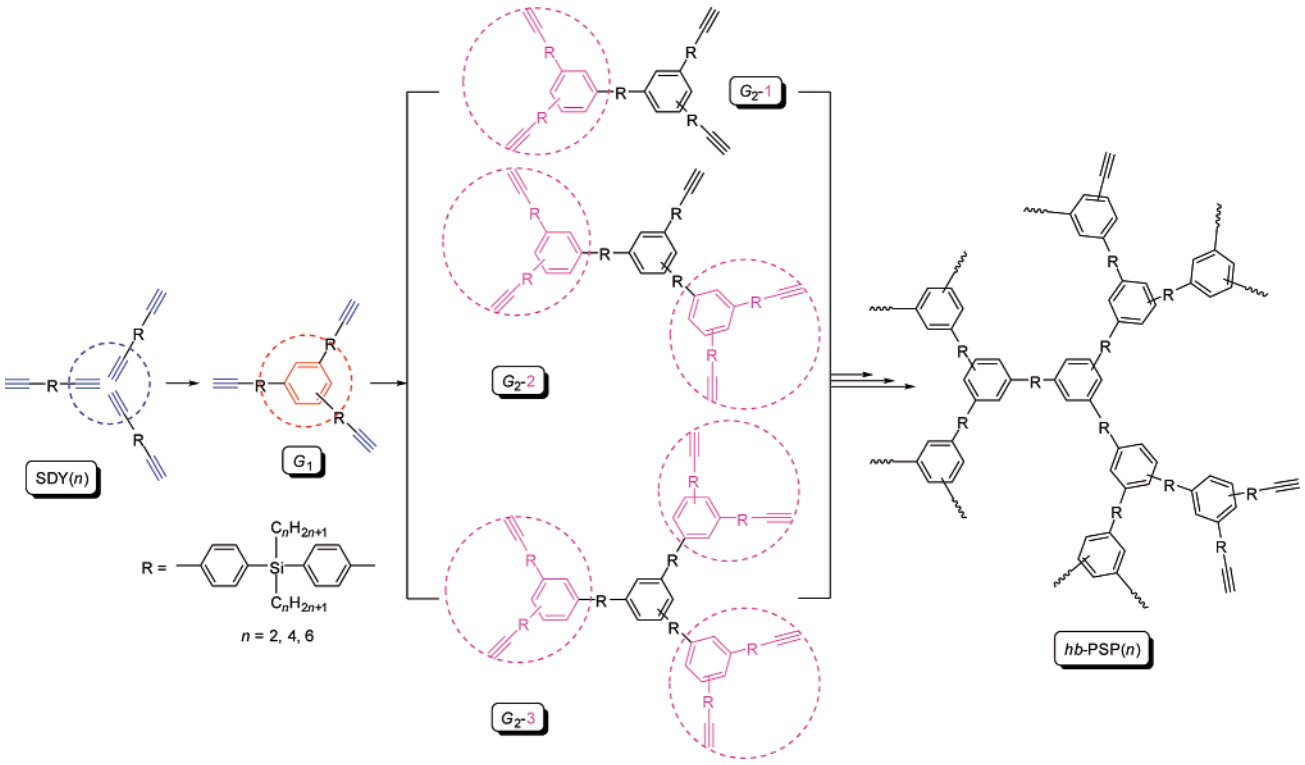

According to the results of the spectroscopic analyses and model reactions, the *hb*-PSPs contain three basic structures, namely, D, L, and T units (Table 7). The number of protons from the newly formed benzene rings is 3 for all three different units, whereas the numbers of protons from the unreacted triple bonds are 0, 1, and 2 for the D, L, and T units, respectively. Assuming that the numbers of D, L, and T units are respectively N_D, N_L, and N_T, we can get the following equations:

$$N_{Ph} = 3N_D + 3N_L + 3N_T \quad (2)$$

$$N_{UT} = 0N_D + 1N_L + 2N_T \quad (3)$$

Here N_{Ph} is the total number of protons from the newly formed benzene rings, and N_{UT} is the number of unreacted triple bonds. Because the total number of protons of the newly formed benzene rings is equal to that of the reacted triple bonds, the following relationships can be established:

$$N_{Ph} = N_{RT} \quad (4)$$

$$\frac{N_{UT}}{N_{RT}} = \frac{N_{UT}}{N_{Ph}} = \frac{0N_D + 1N_L + 2N_T}{3N_D + 3N_L + 3N_T} \quad (5)$$

Here N_{RT} is the number of reacted triple bonds. Assuming that no side reactions and no loop formation occur in the polymerization, we can draw a conclusion that, in one polymer, the number of T units is always larger than that of D units by 2 (i.e., $N_T = N_D + 2$). The ideal growth patterns of D, T, and L units in the polymer are given in Table 8 as an example to support this conclusion. We can see that the number of T units is larger than that of D units by 2 in all species. Examples of some structures given in Table 8 are shown in Chart S1 (Supporting Information). The above conclusion can be applied to not only the ideal growth pattern but also all other patterns. If the molecular weights of the polymers are small or the numbers of their T and D units are not big enough, this difference cannot be neglected. We therefore get the following general equation

$$N_T = N_D + 2N_P \quad (6)$$

where N_P is the total number of hyperbranched polymers. Together with eq 5, N_{UT} and N_{Ph} can be related by eq 7:

$$\frac{N_{UT}}{N_{RT}} = \frac{N_{UT}}{N_{Ph}} = \frac{N_L + 2N_T}{3N_L + 3(N_T - 2N_P) + 3N_T} = \frac{N_L + 2N_T}{3N_L + 6N_T - 6N_P} > \frac{N_L + 2N_T}{3N_L + 6N_T} = \frac{1}{3} \quad (7)$$

According to eq 7, further deductions can be carried out as follows:

$$N_{RT} < 3N_{UT} \quad (8)$$

$$\frac{N_{UT}}{N_{TT}} = \frac{N_{UT}}{N_{RT} + N_{UT}} > \frac{N_{UT}}{3N_{UT} + N_{UT}} = \frac{1}{4} \quad (9)$$

Here N_{TT} is the total number of triple bonds from the monomers. Thus, the molar ratio of the unreacted triple bonds to the total triple bonds from the monomers is larger than $^1/_4$, indicating that more than 25% of the triple bonds should be left after polycyclotrimerization, under the assumption that no loops are formed (eq 9). If some loops are formed in the polymerization reaction, the number will become smaller than 25%.

According to the ^{1}H NMR spectra of the polymers, the fraction (p) of the triple bonds that has been transformed into benzene rings can be estimated from eq 10:

$$p = \frac{N_{RT}}{N_{TT}} = \frac{A_{Ph} - \frac{A_{alkyl}}{4n+2} \times 8}{\frac{A_{alkyl}}{4n+2} \times 2} = \frac{(2n+1)A_{Ph} - 4A_{alkyl}}{A_{alkyl}} \quad (10)$$

Scheme 7

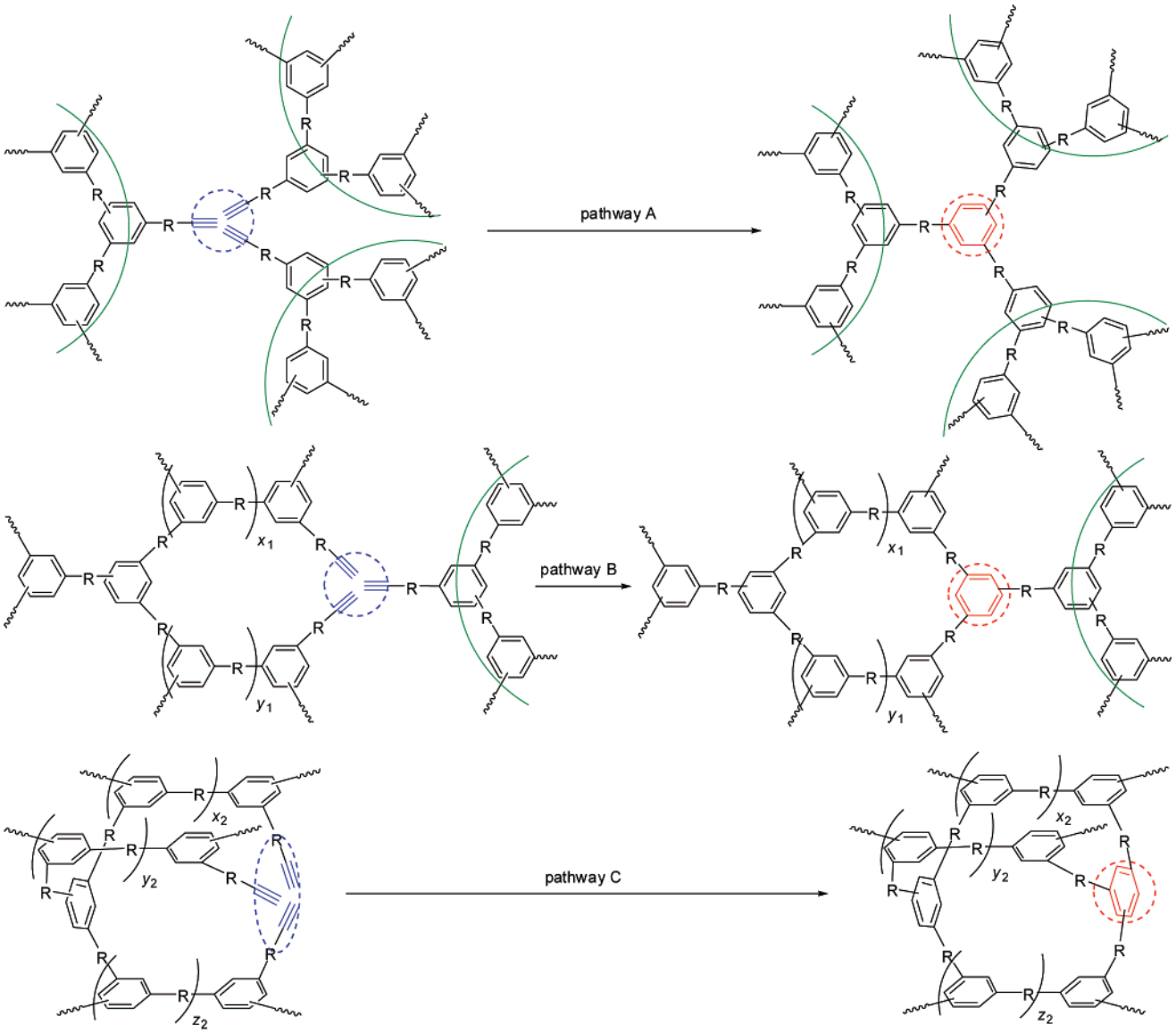

Table 7. Dendritic, Linear, and Terminal Units in *hb*-PSP[a]

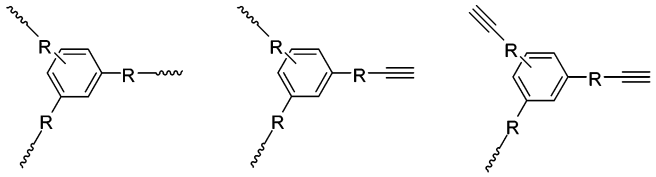

	dendritic unit (*D*)	linear unit (*L*)	terminal unit (*T*)
n_{Ph}[b]	3	3	3
$n_{C\equiv CH}$[c]	0	1	2

[a] R = $(C_6H_4)_2Si(C_nH_{2n+1})_2$; n = 2, 4, 6. [b] Number of protons of a newly formed benzene ring. [c] Number of protons of unreacted triple bond(s).

where A_{Ph} is the integrated area of the resonance peaks from all the benzene rings in the polymer, A_{alkyl} is the integral of the aliphatic resonance peaks, and n represents the number of carbon atoms in the alkyl chain (2, 4, or 6). The value from the newly formed benzene rings represents the number of reacted triple bonds (N_{RT}). This integral equals to the difference between the area from all the benzene rings in the polymers and that from the original benzene rings in the monomers. The total number of triple bonds (N_{TT}) is two times as large as that of the monomers, which can be indirectly calculated from the integrated area of the alkyl chains (eq 10). Most of the polymerizations show almost 75% triple bond conversion, in good agreement with the above theoretical analysis. We have assumed that no loops are formed; however, such a probability cannot be totally excluded.

Table 8. Ideal Growth Patterns of Dendritic, Terminal, and Linear Units in Diyne Polycyclotrimerization[a]

	(n_D, n_T, n_L)				
n_L	G_1	G_2	G_3	G_4	G_x
0		(1, 3, 0)	(4, 6, 0)	(10, 12, 0)	$(3 \times 2^{x-2} - 2, 3 \times 2^{x-2}, 0)$
1		(0, 2, 1)	(3, 5, 1)	(9, 11, 1)	$(3 \times 2^{x-2} - 2 - 1, 3 \times 2^{x-2} - 1, 1)$
0		(0, 2, 0)	(3, 5, 0)	(9, 11, 0)	$(3 \times 2^{x-2} - 2 - 1, 3 \times 2^{x-2} - 1, 0)$
2			(2, 4, 2)	(8, 10, 2)	$(3 \times 2^{x-2} - 2 - 2, 3 \times 2^{x-2} - 2, 2)$
1			(2, 4, 1)	(8, 10, 1)	$(3 \times 2^{x-2} - 2 - 2, 3 \times 2^{x-2} - 2, 1)$
0			(2, 4, 0)	(8, 10, 0)	$(3 \times 2^{x-2} - 2 - 2, 3 \times 2^{x-2} - 2, 0)$
3			(1, 3, 3)	(7, 9, 3)	$(3 \times 2^{x-2} - 2 - 3, 3 \times 2^{x-2} - 3, 3)$
2			(1, 3, 2)	(7, 9, 2)	$(3 \times 2^{x-2} - 2 - 3, 3 \times 2^{x-2} - 3, 2)$
1			(1, 3, 1)	(7, 9, 1)	$(3 \times 2^{x-2} - 2 - 3, 3 \times 2^{x-2} - 3, 1)$
0				(7, 9, 0)	$(3 \times 2^{x-2} - 2 - 3, 3 \times 2^{x-2} - 3, 0)$
4				(6, 8, 4)	$(3 \times 2^{x-2} - 2 - 4, 3 \times 2^{x-2} - 4, 4)$
3				(6, 8, 3)	$(3 \times 2^{x-2} - 2 - 4, 3 \times 2^{x-2} - 4, 3)$
2				(6, 8, 2)	$(3 \times 2^{x-2} - 2 - 4, 3 \times 2^{x-2} - 4, 2)$
1				(6, 8, 1)	$(3 \times 2^{x-2} - 2 - 4, 3 \times 2^{x-2} - 4, 1)$
0				(6, 8, 0)	$(3 \times 2^{x-2} - 2 - 4, 3 \times 2^{x-2} - 4, 0)$
5				(5, 7, 5)	$(3 \times 2^{x-2} - 2 - 5, 3 \times 2^{x-2} - 5, 5)$
4				(5, 7, 4)	$(3 \times 2^{x-2} - 2 - 5, 3 \times 2^{x-2} - 5, 4)$
3				(5, 7, 3)	$(3 \times 2^{x-2} - 2 - 5, 3 \times 2^{x-2} - 5, 3)$
2				(5, 7, 2)	$(3 \times 2^{x-2} - 2 - 5, 3 \times 2^{x-2} - 5, 2)$
1				(5, 7, 1)	$(3 \times 2^{x-2} - 2 - 5, 3 \times 2^{x-2} - 5, 1)$
0				(5, 7, 0)	$(3 \times 2^{x-2} - 2 - 5, 3 \times 2^{x-2} - 5, 0)$
6				(4, 6, 6)	$(3 \times 2^{x-2} - 2 - 6, 3 \times 2^{x-2} - 6, 6)$
5				(4, 6, 5)	$(3 \times 2^{x-2} - 2 - 6, 3 \times 2^{x-2} - 6, 5)$
4				(4, 6, 4)	$(3 \times 2^{x-2} - 2 - 6, 3 \times 2^{x-2} - 6, 4)$
3				(4, 6, 3)	$(3 \times 2^{x-2} - 2 - 6, 3 \times 2^{x-2} - 6, 3)$
2				(4, 6, 2)	$(3 \times 2^{x-2} - 2 - 6, 3 \times 2^{x-2} - 6, 2)$
1				(4, 6, 1)	$(3 \times 2^{x-2} - 2 - 6, 3 \times 2^{x-2} - 6, 1)$
0					$(3 \times 2^{x-2} - 2 - 6, 3 \times 2^{x-2} - 6, 0)$
...					...
y					$(3 \times 2^{x-2} - 2 - y, 3 \times 2^{x-2} - y, y)$
$y-1$					$(3 \times 2^{x-2} - 2 - y, 3 \times 2^{x-2} - y, y-1)$
$y-2$					$(3 \times 2^{x-2} - 2 - y, 3 \times 2^{x-2} - y, y-2)$
...					...
1					$(3 \times 2^{x-2} - 2 - y, 3 \times 2^{x-2} - y, 1)$

[a] Growth of each generation G_x is based on the assumption that the generation G_{x-1} has been perfectly grown and no loops are formed in the polymerization. Symbols: x = number of generations, $y = 3 \times 2^{x-3}$, n_D = number of dendritic units, n_T = number of terminal units, and n_L = number of linear units.

One of the most important parameters for a hyperbranched polymer is its DB value, which are defined by the following equations:

$$f_D = \frac{N_D}{N_D + N_T + N_L} \tag{11}$$

$$f_T = \frac{N_T}{N_D + N_T + N_L} \tag{12}$$

$$f_L = \frac{N_L}{N_D + N_T + N_L} \tag{13}$$

$$f_T + f_D + f_L = 1 \tag{14}$$

$$DB = \frac{N_D + N_T}{N_D + N_T + N_L} = f_D + f_T \tag{15}$$

where f_D, f_T, and f_L are the fractions of D, T, and L units. Unfortunately, the NMR signals of the newly formed benzene rings in the D, T, and L units of the polymers cannot be easily distinguished from each other, which are overlapping with the resonances of the original benzene rings from the monomers. It is thus difficult to calculate the ratio of D, T, or L units, which in turn makes it difficult to directly calculate the DB values. We can, however, establish some important relationships between the DB and other characteristic parameters.

As we know, the remaining triple bonds in the polymers come from two parts: one is originated from the T unit and the other is from the L unit. Therefore, N_T, N_L, and p can be related by eq 16:

$$2N_T + N_L = 2n_m(1 - p) \tag{16}$$

where n_m is the number of monomers. Because no small molecules are eliminated in the polymerization, the degree of polymerization (DP_n) can be easily calculated according to eq 17:

$$\frac{n_m}{N_p} = \frac{M_n}{M_m} = DP_n \tag{17}$$

where M_m is the molecular weight of the monomer. Together with eqs 6 and 16 and assuming that no loops are formed, we can get eq 18 through a simple mathematical treatment:

$$\frac{2N_T + N_L}{N_T - N_D} = DP_n(1 - p) \tag{18}$$

Together with eqs 11−13, eq 18 can be transformed into eq 19

$$\frac{2f_T + f_L}{f_T - f_D} = DP_n(1 - p) \tag{19}$$

where DP_n and p can be obtained from GPC and NMR analyses, respectively. For example, when $DP_n = 21$ and $p = 0.697$, f_L

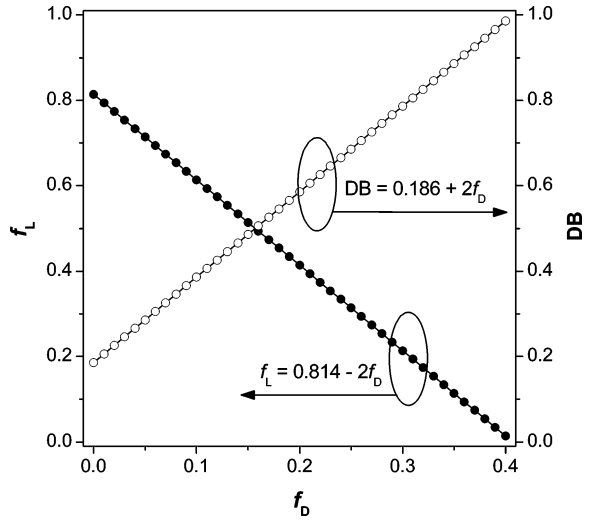

Figure 5. Variations of the fraction of linear unit (f_L) and the degree of branching (DB) with the fraction of dendritic unit (f_D; sample taken from Table 5, no. 6).

and DB can be expressed as a function of f_D by eqs 20 and 21, respectively:

$$f_L = 0.814 - 2f_D \tag{20}$$

$$DB = 1 - f_L = 0.186 + 2f_D \tag{21}$$

The relationships described in eqs 20 and 21 are expressed by the fitting curves in Figure 5. We can see that the DB is a first-order incremental function of f_D. When f_D is, for example, 0.2, which means only two out of 10 newly formed benzene rings are D units in the polycyclotrimerization, the associated DB value is 0.59, which is already higher than those of the conventional hyperbranched polymers prepared by the polycondensations of AB_2-type monomers.[6−8]

While the above analyses are from the chemistry point of view, mathematical treatments can also be used to assist the chemical structure analyses. We have proven that our polymers are formed via the [2 + 2 + 2] cyclotrimerization mechanism. If we make the same assumption that no loops are formed in the polycyclotrimerization, we will find that DP_n is always an odd number (Table S1 in the Supporting Information) and its relationship with the number of newly formed benzene rings (N_b) can be related by eq 22:

$$DP_n = 2N_b + 1 \tag{22}$$

where N_b is the number of newly formed benzene rings. Through further mathematical deductions, the relationship between the extent of triple bond conversion (p) and N_b can be expressed by eq 23:

$$p = \frac{3N_b}{4N_b + 2} \tag{23}$$

Figure 6 illustrates the relationships between these parameters. We can clearly see that the extent of triple bond conversion rapidly increases with increasing N_b and levels off at 0.75. This is consistent with the conclusion obtained from the chemical structure analysis, in which less than 75% of the triple bonds have been reacted. For example, if N_b is 10, DP_n and p will be 21 and 0.714, respectively, which agree with the previous results ($DP_n = 21$ and $p = 0.697$) obtained from a sample we have chosen for the DB analysis.

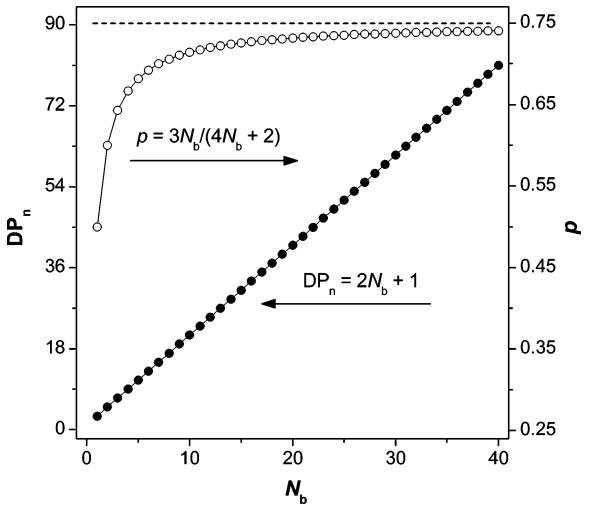

Figure 6. Variations of the degree of polymerization (DP_n) and the extent of triple bond conversion (p) with the number of newly formed benzene rings (N_b).

To visualize the insights gained from the structural analyses, computational simulation is conducted. The polymer structure is modeled using the Materials Studio program,[37] where the lowest energy of each generation is used to generate the next generation. Similar to the structural analysis, we chose an *hb*-PSP(4) comprising 21 monomers for the analysis in the computer simulation. According to eq 22, 10 new benzene rings are formed by the polymerization reaction. The p value for this polymer is 0.697, with 12.6 triple bonds unreacted. Because the calculated molar ratio of 1,3,5- to 1,2,4-TPB for this sample is ~1.0:1.7, we can further conclude that 3.7 and 6.3 in the 10 newly formed benzene rings are 1,3,5- and 1,2,4-TPBs, respectively. Detailed procedures for the model construction are described in the Supporting Information. The obtained two- and three-dimensional topological modeling structures are shown in Figure 7. It can be seen that when 21 monomers are reacted, 12 triple bonds are left and 10 new benzene rings are formed. Four of them are 1,3,5-TPB rings, and the remaining six are 1,2,4-TPB rings.

According to the computer simulation, we can get the following information from the modeling study:

$$p = 30/42 = 0.714 \tag{24}$$

$$N_D = 3, \quad N_T = 5, \quad N_L = 2 \tag{25}$$

$$DB = \frac{N_D + N_T}{N_D + N_T + N_L} = f_D + f_T = 0.3 + 0.5 = 0.8 \tag{26}$$

The computer-generated model gives an f_D value of 0.3, which corresponds to a DB value of 0.8. This value is in good agreement with the one (0.79) calculated from eq 21. The results from the model study and the spectroscopic analysis are thus consistent. The modeling gives us a tool to calculate the DB and to gain more insights into the real topological structures of the hyperbranched polymers.

Thermal and Optical Properties. Thermal properties of the hyperbranched polymers are evaluated by thermogravimetric analysis (TGA). All the *hb*-PSPs exhibit outstanding thermal stability, with their degradation temperatures (T_d's) being ≥445 °C (Figure 8 and Table 9). With an increase in the alkyl chain length, the resistance of the polymers toward thermolysis decreases. This is understandable as the alkyl chains readily decompose at high temperatures. The polymers with shorter alkyl chains lose merely 5% of their weights at a temperature

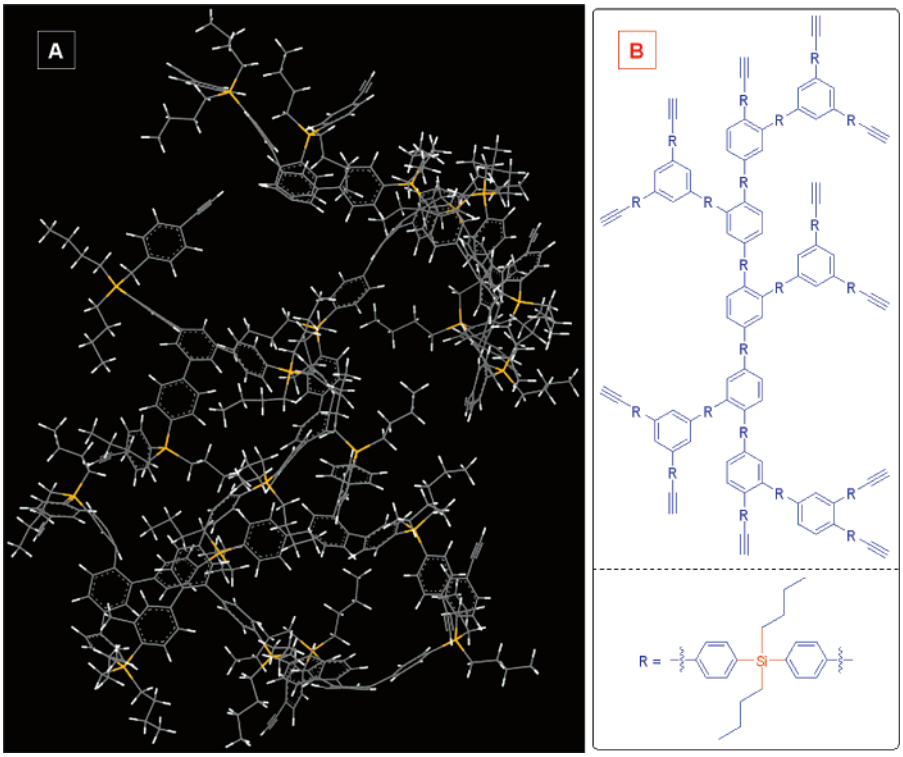

Figure 7. (A) Three-dimensional topological structures of *hb*-PSP(4) simulated by Materials Studio program and (B) its associated two-dimensional structure.

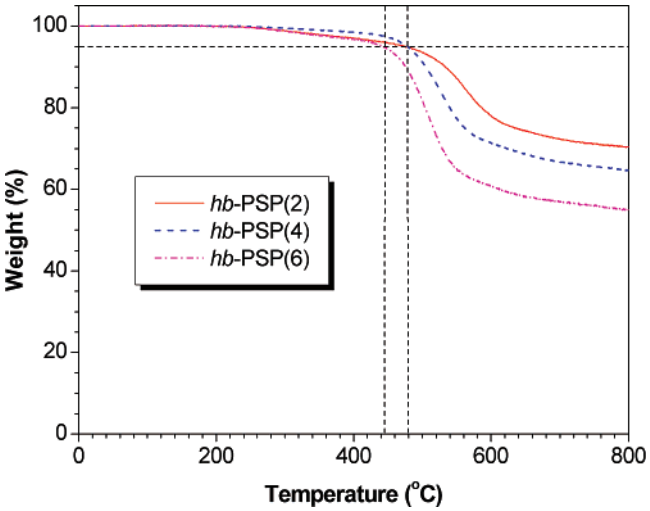

Figure 8. TGA thermograms of *hb*-PSP(2) (sample taken from Table 6, no. 3), *hb*-PSP(4) (Table 6, no. 7) and *hb*-PSP(6) (Table 5, no. 12) recorded under nitrogen at a heating rate of 20 °C.

Table 9. Thermal and Optical Properties of *hb*-PSP(*n*)[a]

	λ_{ab} (nm)[b]	λ_{em} (nm)[c]	Φ_F (%)[d]	T_d (°C)[e]	W_r (%)[f]
TPB[g]	252.9	356.8	5.3		
hb-PSP(2)	266.6	380.8	6.9	480	71
hb-PSP(4)	267.6	380.0	7.0	480	65
hb-PSP(6)	266.3	380.0	6.9	445	55

[a] Thermal and optical measurements carried out in the solid and solution states, respectively. [b] Absorption maximum. [c] Emission maximum. [d] Quantum yield estimated using 9,10-diphenylanthracene as standard (Φ_F = 90% in cyclohexane). [e] Temperature for 5% weight loss. [f] Weight of residue after pyrolysis at 800 °C. [g] 1,2,4- and 1,3,5-isomeric mixtures.

as high as 480 °C and carbonize in high yields (up to 70%) when pyrolyzed at 800 °C. These results are consistent with their polyphenylene structures, in which their branch units are knitted together by stable aromatic rings. The thermal stabilities

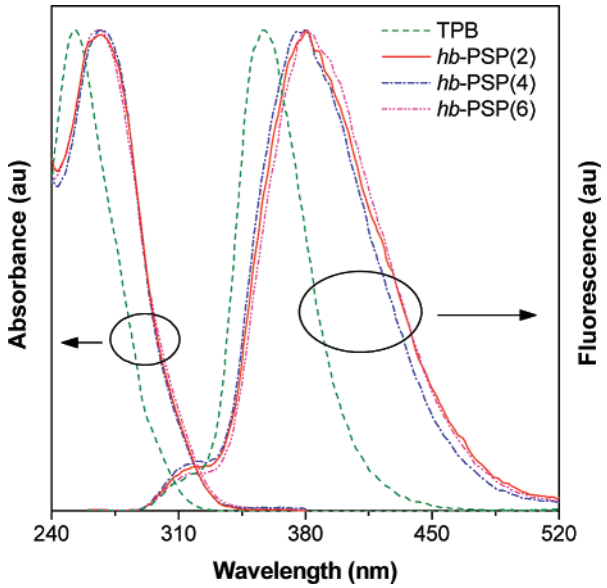

Figure 9. UV and PL spectra of THF solutions of *hb*-PSP(2) (sample taken from Table 2, no. 6), *hb*-PSP(4) (Table 5, no. 4) and *hb*-PSP(6) (Table 2, no. 15). The spectrum of a mixture of 1,2,4- and 1,3,5-TPBs (~2:1 by mole) is shown for comparison. Concentration: 10 μM; excitation wavelength: 257 nm.

of the polymers in air are somewhat lower (T_d = 386−423 °C) than those under nitrogen because of the involvement of oxidative thermolysis (Figure S1, Supporting Information).

The UV and photoluminescence (PL) spectra of the THF solutions of *hb*-PSPs are shown in Figure 9. The spectra of a mixture of 1,2,4- and 1,3,5-TPBs are shown for comparison. The TPB mixture shows an absorption peak at ~253 nm, while the absorptions of *hb*-PSPs are located at a longer wavelength of ~267 nm, indicative of a more conjugated electronic structure in the hyperbranched polymers. Similar red-shifts are observed in the PL spectra. Upon photoexcitation, the *hb*-PSPs emit a

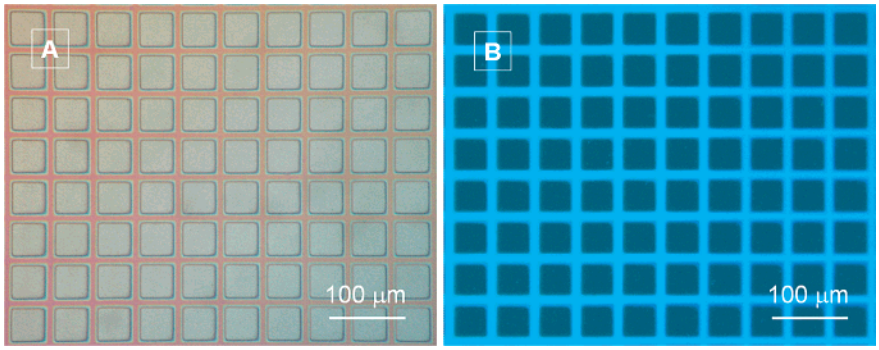

Figure 10. Three-dimensional negative-tone photoresist patterns generated by photo-cross-linking of *hb*-PSP(6) (sample taken from Table 2, no. 15); photos taken under (A) normal lighting and (B) UV illumination.

violet-blue light of ~380 nm, while the PL spectrum of the TPB mixture is peaked at a shorter wavelength of ~357 nm. The fluorescence quantum yields of the polymers in THF are 6.5−7.0%, higher than that of the TPB mixture (5.3%; Table 9). The polymers emit strong light even after being fabricated into thin solid films, thanks to its nonplanar molecular structure, which has effectively inhibited the formation of the excimeric species in the solid state.[38]

Since the *hb*-PSPs are emissive in the solid state and possess many cross-linkable triple bonds on their peripheries, we explored their potential use as fluorescent imaging materials. The polymers can form uniform, tough films by spin-coating their 1,2-dichloroethane solutions onto silicon wafers. Exposure of a thin solid film of *hb*-PSP(6) to UV irradiation through a negative copper mask readily cross-links the exposed regions, whereas the unexposed regions are removed by a development process using 1,2-dichloroethane as the developing agent. This leads to the formation of a photoresist pattern with sharp edges (Figure 10). As can be seen from Figure 10B, the photo-cross-linked pattern emits a strong blue light under UV illumination. This makes the polymers promising candidate materials for photoimaging applications.

Conclusions

In this work, we have successfully synthesized a group of soluble and processable *hb*-PSPs by the polycyclotrimerization of A_2-type monomers initiated by a single-component catalyst of $TaBr_5$. The A_2 system enjoys such advantages as easy monomer synthesis and simple polymerization procedure, in comparison to the traditional AB_2 and $A_2 + B_3$ systems. The model reactions confirm that the *hb*-PSPs are formed via a [2 + 2 + 2] cyclotrimerization mechanism. The spectroscopic analyses assisted by the mathematical modeling reveal that ~75% of the triple bonds have been cyclotrimerized into benzene rings. The relationship between DB and f_D is established. To overcome the difficulty in calculating the DB values of the polymers and to gain insights into their real topological structures, computational simulation is carried out, which offers results well consistent with the experimental data. The *hb*-PSPs are thermally stable, losing little weights at T_d's up to 480 °C and keeping up to 71% of their original weights after pyrolysis at 800 °C. The polymers are readily photo-cross-linked, generating well-resolved fluorescent photoimages.

Experimental Section

General Information. Toluene, hexane, dioxane, and THF were distilled from sodium benzophenone ketyl immediately prior to use. DCM was distilled over calcium hydride. Triethylamine was distilled under nitrogen and stored over sodium hydroxide in a dark, cold place before use. Tantalum(V) bromide, tetraphenyltin, dichlorobis(triphenylphosphine)palladium(II), copper(I) iodide, triphenylphosphine, and other chemicals and solvents were all purchased from Aldrich and used as received without further purification.

The M_n, M_w and M_w/M_n or PDI values of the polymers were estimated by a Waters Associates GPC system in THF using a set of monodisperse linear polystyrenes as calibration standards. IR spectra were recorded on a Perkin-Elmer 16 PC FTIR spectrophotometer. ^1H and ^{13}C NMR spectra were measured on a Bruker ARX 300 NMR spectrometer using chloroform-*d* or DCM-d_2 as solvent and tetramethyl-silane (TMS) as internal reference. UV absorption spectra were measured on a Milton Ray Spectronic 3000 array spectrophotometer. PL spectra were recorded on a Perkin-Elmer LS 55 spectrofluorometer. Mass spectra were recorded on a GCT Premier CAB 048 mass spectrometer. TGA measurements were carried out on a Perkin-Elmer TGA 7 analyzer at a heating rate of 20 °C/min.

Monomer Synthesis. Diyne monomers of SDY(*n*) were prepared by a three-step reaction protocol according to the synthetic routes shown in Scheme 1. Typical experimental procedures for the synthesis of the monomers are given below.

(4-Bromophenylethynyl)trimethylsilane (2). Into a round-bottomed flask equipped with a septum and a stirring bar was placed 11.32 g (40 mmol) of 1-bromo-4-iodobenzene (**1**). The flask was put into a glovebox and 281 mg (0.4 mmol) of dichlorobis(triphenylphosphine)palladium(II), 19 mg (0.1 mmol) of CuI, and 26 mg (0.1 mmol) of triphenylphosphine were thus added. Afterward, 100 mL of dried triethylamine and 5.65 mL (40 mmol) of trimethylsilylacetylene was injected into the flask by syringes under stirring. The mixture was stirred at room temperature for 2 h. The formed precipitates were filtered and washed with diethyl ether. The solutions were combined and the solvent was evaporated. The crude product was purified by a silica gel column chromatography using hexane as eluent. A white powdery product was obtained in 97% yield (9.82 g). IR (thin film), ν (cm^{-1}): 2962, 2899 (CH_3 stretching), 2158 (C≡C stretching), 1893 (overtone band, disubstituted benzene ring), 1245 (Si−CH_3 bending), 845 (Si−C stretching). ^1H NMR (300 MHz, $CDCl_3$), δ (TMS, ppm): 7.42 (d, 2H, Ar−*H* ortho to Br), 7.31 (d, 2H, Ar−*H* meta to Br), 0.24 (s, 9H, Si−C*H*$_3$). ^{13}C NMR (75 MHz, $CDCl_3$), δ (ppm): 133.2 (aromatic carbon meta to Br), 131.3 (aromatic carbon ortho to Br), 122.6 (aromatic carbon linked with Br), 122.0 (aromatic carbon para to Br), 103.8 (acetylenic carbon linked with aromatic ring), 95.5 (acetylenic carbon linked with Si), 0.01 (Si−*C*H$_3$).

Bis(4-ethynylphenyl)diethylsilane [SDY(2)]. Into a nitrogen-flushed, round-bottomed flask equipped with a septum and a stirring bar was placed 2.53 g (10.0 mmol) of **2** and 100 mL of THF. The flask was cooled at −78 °C and 4.2 mL of 2.5 M (10.5 mmol) *n*-butyllithium in hexane was added dropwise under vigorous stirring. After stirring at −78 °C for 2 h, 0.75 mL (5.0 mmol) of dichlorodiethylsilane was added dropwise. The mixture was then warmed to room temperature. After solvent evaporation, the colorless liquid was dissolved in DCM and washed with water three times. The organic layers were combined. After removal of solvent, the intermediate of bis[4-(2-trimethylsilylethynyl)phenyl]diethyl-

silane (**3**) was directly placed in another round-bottomed flask equipped with a septum and a stirring bar. Methanol (350 mL) and KOH (140 mg, 2.5 mmol) were then added. The mixture was stirred at room temperature for 8 h and then poured into 1000 mL of 1 M HCl solution. The mixture was extracted by DCM three times. The organic layers were combined. After the solvent was removed under reduced pressure, the crude product was purified by silica gel column using a mixture of hexane and chloroform (3:1 v/v) as eluent. Colorless liquid of SDY(2) was obtained in 83.8% yield (4.2 mmol). IR (thin film), ν (cm^{-1}): 3296 (≡C−H stretching), 3067, 3016 (Ar−H stretching), 2956, 2875 (C−H stretching in alkyl chain), 2108 (C≡C stretching), 1921, (overtone band, substituted benzene ring), 1594, 1537, 1488 (C═C ring stretching), 1100 (Si−Ph stretching), 823 (Si−C stretching). ^{1}H NMR (300 MHz, CD_2Cl_2), δ (TMS, ppm): 7.44 (m, 8H, Ar−H), 3.15 (s, 2H, ≡C−H), 1.02 [m, 4H, Si(CH_2CH_3)$_2$], 0.98 (m, 6H, Si(CH_2CH_3)$_2$). ^{13}C NMR (75 MHz, CD_2Cl_2), δ (ppm): 137.6 (aromatic carbon linked with Si), 135.2 (aromatic carbon ortho to Si), 131.6 (aromatic carbon meta to Si), 123.2 (aromatic carbon para to Si), 84.0 (acetylenic carbon linked with aromatic ring), 78.2 (acetylenic carbon linked with H), 7.6 [Si(CH_2CH_3)], 4.1 [Si(CH_2CH_3)]. HRMS (EI): *m*/*e* 288.1337 (calcd 288.1334).

Bis(4-ethynylphenyl)dibutylsilane [SDY(4)]. This monomer was prepared according to the procedures similar to those used for the preparation of SDY(2) described above, as a colorless liquid; yield: 84.8%. IR (thin film), ν (cm^{-1}): 3299 (≡C−H stretching), 3067, 3014 (Ar−H stretching), 2956, 2871 (C−H stretching in alkyl chain), 2108 (C≡C stretching), 1920, (overtone band, substituted benzene ring), 1594, 1537, 1487 (C═C ring stretching), 1100 (Si−Ph stretching), 822 (Si−C stretching). ^{1}H NMR (300 MHz, CD_2Cl_2), δ (TMS, ppm): 7.47 (m, 8H, Ar−H), 3.16 (s, 2H, ≡C−H), 1.36 [m, 8H, Si($CH_2CH_2CH_2-CH_3$)$_2$], 1.12 [m, 4H, Si($CH_2CH_2-CH_2CH_3$)$_2$], 0.88 [m, 6H, Si($CH_2CH_2CH_2CH_3$)$_2$]. ^{13}C NMR (75 MHz, CD_2Cl_2), δ (ppm): 138.2 (aromatic carbon linked with Si), 135.2 (aromatic carbon ortho to Si), 131.6 (aromatic carbon meta to Si), 123.2 (aromatic carbon para to Si), 84.0 (acetylenic carbon linked with aromatic ring), 78.3 (acetylenic carbon linked with H), 27.3 [Si($CH_2CH_2CH_2CH_3$)$_2$], 26.5 [Si($CH_2-CH_2CH_2CH_3$)$_2$], 14.2 [Si($CH_2CH_2CH_2CH_3$)$_2$], 12.5 [Si($CH_2CH_2CH_2CH_3$)$_2$]. HRMS (CI): *m*/*e* 345.2038 [(M + 1)$^+$, calcd 345.1960].

Bis(4-ethynylphenyl)dihexylsilane [SDY(6)]. This monomer was prepared by the procedures similar to those used for the preparation of SDY(2). Colorless liquid; yield: 84.2%. IR (thin film), ν (cm^{-1}): 3302 (≡C−H stretching), 3067, 3014 (Ar−H stretching), 2956, 2871 (C−H stretching in alkyl chain), 2109 (C≡C stretching), 1919 (overtone band, substituted benzene ring), 1594, 1537, 1487 (C═C ring stretching), 1100 (Si−Ph stretching), 822 (Si−C stretching). ^{1}H NMR (300 MHz, CD_2Cl_2), δ (TMS, ppm): 7.44 (m, 8H, Ar−H), 3.15 (s, 2H, ≡C−H), 1.26 [m, 16H, Si($CH_2CH_2CH_2CH_2CH_3$)$_2$], 1.07 [m, 4H, Si($CH_2CH_2CH_2CH_2-CH_2CH_3$)$_2$], 0.84 [m, 6H, Si($CH_2CH_2CH_2CH_2CH_2CH_3$)$_2$]. ^{13}C NMR (75 MHz, CD_2Cl_2), δ (ppm): 138.3 (aromatic carbon linked with Si), 135.3 (aromatic carbon ortho to Si), 131.6 (aromatic carbon meta to Si), 123.4 (aromatic carbon para to Si), 84.0 (acetylenic carbon linked with aromatic ring), 78.3 (acetylenic carbon linked with H), 33.7 [Si($CH_2CH_2CH_2CH_2CH_2CH_3$)$_2$], 32.1 [Si($CH_2CH_2-CH_2CH_2CH_2CH_3$)$_2$], 23.8 [Si($CH_2CH_2CH_2CH_2CH_2CH_3$)$_2$], 23.2 [Si-($CH_2CH_2CH_2CH_2CH_2-CH_3$)$_2$], 14.4 [Si($CH_2CH_2CH_2CH_2CH_2CH_3$)$_2$], 12.6 [Si($CH_2CH_2CH_2CH_2CH_2CH_2CH_3$)$_2$]. HRMS (CI): *m*/*e* 401.2678 [(M + 1)$^+$, calcd 401.2586].

Polymerization Reactions. All the polymerization reactions were carried out under nitrogen using the standard Schlenk technique in a vacuum line system or an inert atmosphere glovebox. Typical experimental procedures for the polycyclotrimerization of SDY(2) are given below.

To a thoroughly baked and carefully evacuated 15 mL Schlenk tube with a three-way stopcock on the sidearm was placed 8.7 mg (0.015 mmol) of $TaBr_5$ under nitrogen in a glovebox. Freshly distilled toluene (2.0 mL) was then injected into the tube using a hypodermic syringe. After this mixture was stirred for 5 min, a solution of 86.5 mg (0.30 mmol) of SDY(2) in 1.0 mL of toluene was injected. The resultant mixture was stirred at room temperature under nitrogen for 8 h, and the polymerization was then quenched by the addition of a small amount of methanol. The solution was added dropwise to 300 mL of methanol via a cotton filter under stirring. The precipitate was allowed to stand overnight and then collected by filtration. The polymer was washed with methanol and dried under vacuum at room temperature to a constant weight.

Characterization Data for *hb*-PSP(2). The compound was obtained as a white powder; yield: 84.4%; M_w 11900; M_w/M_n 2.6 (Table 2, no. 6). IR (thin film), ν (cm^{-1}): 3294 (≡C−H stretching), 3063, 3016 (Ar−H stretching), 2955, 2874 (C−H stretching in alkyl chain), 2107 (C≡C stretching), 1918 (overtone band, substituted benzene ring), 1594, 1542, 1499 (C═C ring stretching), 1111 (Si−Ph stretching), 823 (Si−C stretching). ^{1}H NMR (300 MHz, CD_2Cl_2), δ (TMS, ppm): 6.80−8.00 (Ar−H), 3.15 (≡C−H), 0.5−1.4 [Si(CH_2CH_3)$_2$]. ^{13}C NMR (75 MHz, CD_2Cl_2), δ (ppm): 118.0−145.0 (aromatic carbons), 83.8 (*C*≡CH), 78.0 (C≡*C*H), 7.4 [Si-(CH_2CH_3)], 4.1 [Si(CH_2CH_3)].

***hb*-PSP(4).** This was obtained as a white powder; yield: 85.6%; M_w 13200; M_w/M_n 2.3 (Table 5, no. 4). IR (thin film), ν (cm^{-1}): 3301 (≡C−H stretching), 3063, 3016 (Ar−H stretching), 2955, 2870 (C−H stretching in alkyl chain), 2104 (C≡C stretching), 1917 (overtone band, substituted benzene ring), 1594, 1542, 1499 (C═C ring stretching), 1111 (Si−Ph stretching), 822 (Si−C stretching). ^{1}H NMR (300 MHz, CD_2Cl_2), δ (TMS, ppm): 6.80−8.40 (Ar−H), 3.15 (≡C−H), 0.3−1.8 [Si($CH_2CH_2CH_2CH_3$)$_2$]. ^{13}C NMR (75 MHz, CD_2Cl_2), δ (ppm): 111.0−144.0 (aromatic carbons), 83.6 (*C*≡CH), 77.8 (C≡*C*H), 26.9 [Si($CH_2CH_2CH_2CH_3$)$_2$], 26.2 [Si($CH_2-CH_2CH_2CH_3$)$_2$], 13.5 [Si($CH_2CH_2CH_2CH_3$)$_2$], 11.9 [Si($CH_2CH_2CH_2-CH_3$)$_2$].

***hb*-PSP(6).** This was obtained as a white powder; yield: 100%; M_w 13500; M_w/M_n 2.1 (Table 2, no. 15). IR (thin film), ν (cm^{-1}): 3303 (≡C−H stretching), 3064, 3016 (Ar−H stretching), 2922, 2855 (C−H stretching in alkyl chain), 2104 (C≡C stretching), 1916 (overtone band, substituted benzene ring), 1594, 1542, 1499 (C═C ring stretching), 1111 (Si−Ph stretching), 822 (Si−C stretching). ^{1}H NMR (300 MHz, CD_2Cl_2), δ (TMS, ppm): 6.70−8.00 (Ar−H), 3.15 (≡C−H), 0.60−1.60 [Si($CH_2CH_2CH_2CH_2CH_2CH_3$)$_2$]. ^{13}C NMR (75 MHz, CD_2Cl_2), δ (ppm): 118.0−145.0 (aromatic carbons), 84.0 (*C*≡CH), 78.1 (C≡*C*H), 33.7 [Si($CH_2CH_2CH_2CH_2-CH_2CH_3$)$_2$], 32.1 [Si($CH_2CH_2CH_2CH_2CH_2CH_3$)$_2$], 24.2 [Si($CH_2CH_2-CH_2CH_2CH_2-CH_3$)$_2$], 23.3 [Si($CH_2CH_2CH_2CH_2CH_2CH_3$)$_2$], 14.6 [Si($CH_2CH_2CH_2CH_2CH_2CH_3$)$_2$], 12.9 [Si($CH_2CH_2CH_2CH_2CH_2-CH_3$)$_2$].

Synthesis of Model Compounds. 1,3,5- and 1,2,4-TPBs were prepared by cyclotrimerization of 0.55 mL (511.5 mg, 5.0 mmol) of phenylacetylene catalyzed by 29.0 mg (0.05 mmol) of $TaBr_5$ in 5.0 mL of toluene. The procedures were similar to that described above. The crude products were purified by silica gel column chromatography using hexane to give TPB mixtures as a white powder. 1,3,5- and 1,2,4-TPBs were separated by recrystallization from ethanol and a mixture of ethanol/hexane (1:1 v/v), respectively. The total isolation yield of the TPBs was 85%. The molar ratio of 1,3,5- to 1,2,4-TPB was ∼1.0:2.0.

Characterization Data for 1,3,5-TPB. IR (thin film), ν (cm^{-1}): 3058, 3033 (Ar−H stretching), 1595, 1576, 1497, 1411 (C═C− ring stretching), 873, 762, 698 (Ar−H bending). ^{1}H NMR (300 MHz, $CDCl_3$), δ (ppm): 7.78 (s, 3H, Ar−H, h), 7.69 (m, 6H, Ar−H, g), 7.47 (m, 6H, Ar−H, f), 7.38 (m, 3H, Ar−H, (e) (the peak assignments were referred to the protons marked in Scheme 4, which were calculated according to the minimized energy of the structure by the MOPAC program installed in the ChemDraw 3D software). ^{13}C NMR (75 MHz, $CDCl_3$), δ (ppm): 142.3, 141.1, 128.8, 127.5, 127.3, 125.2 (aromatic carbons). MS (CI): *m*/*e* 307.1 [(M + 1)$^+$, calcd 307.1].

1,2,4-TPB. IR (thin film), ν (cm^{-1}): 3055, 3025 (Ar−H stretching), 1599, 1575, 1490, 1474 (C═C ring stretching), 756, 697 (Ar−H bending). ^{1}H NMR (300 MHz, $CDCl_3$), δ (ppm): 7.66 (m, 4H, Ar−H, k), 7.47 (m, 3H, Ar−H, j), 7.35 (m, 1H, Ar−H, (i), 7.20 (m, 10H, Ar−H, l) (the peak assignments were referred to the protons marked in Scheme 4, which were calculated according

to the minimized energy of the structure by the MOPAC program installed in the ChemDraw 3D software). ^{13}C NMR (75 MHz, $CDCl_3$), δ (ppm): 141.5, 141.1, 141.0, 140.6, 140.4, 139.5, 131.1, 129.9, 129.8, 129.4, 128.8, 127.9, 127.8, 127.4, 127.1, 126.6, 126.5, 126.1 (aromatic carbons). MS (CI): *m*/*e* 307.1 [$(M + 1)^+$, calcd 307.1].

Decomposition of *hb*-PSPs. The polymers were decomposed by an acid-catalyzed Si−C cleavage reaction. Typical procedures for the decomposition of *hb*-PSP(2) are given below.

To a round-bottom flask equipped with a septum and a stirrer bar was added 89.0 mg of *hb*-PSP(2) (sample taken from Table 6, no. 3) and 50 mL of DCM. After the polymer was dissolved, 5 mL (65 mmol) of CF_3COOH was added dropwise under stirring. After boiling for 96 h, the solution was added slowly to 0.2 M of aqueous solution of sodium carbonate. The organic portion was separated and the aqueous layer was extracted with DCM. The organic layer was collected and washed with deionized water. After evaporation of the solvent, the crude product was purified by a silica gel column using hexane and then hexane/chloroform mixture (1:3 v/v) to give 35 mg of a mixture of 1,3,5- and 1,2,4-TPBs and 26.0 mg of oligomeric species.

Polymers *hb*-PSP(4) (Table 5, no. 6) and *hb*-PSP(6) (Table 4, no.10) were decomposed by the similar procedures. While 39.0 mg of TPBs and 32.0 mg of oligomeric species were obtained from 99.0 mg of *hb*-PSP(4), 48.0 mg of *hb*-PSP(6) was decomposed to give 19.0 mg of TPBs and 12.0 mg of oligomeric species.

Structural Simulation. Molecular modeling programs in the Materials Studio software[37] were used to predict the polymer structures. The model-building strategy is given in detail in the Supporting Information. The sample was taken from Table 5, no. 6, and the following experimentally acquired parameters were used: (1) the M_n of the polymer measured by GPC was ∼7200; (2) the molar ratio of the newly formed 1,2,4- and 1,3,5-TPB units measured by NMR was ∼1.7:1.0; (3) 21 monomers were consumed, which were obtained according to the quotient of the M_n of the polymer and the M_m of the monomer; (4) the *p* value calculated from NMR data was 0.697, suggesting that polymer carries 12.6 unreacted triple bonds. Meanwhile we assumed that no loops had formed in the polymerization reaction.

Interactions in the system are described by a potential *E*, which consists of harmonic bond length, harmonic bond angle, 3-fold tensional, inversion and nonbonding interactions, the last of which can be further subdivided into hydrogen bonding, van der Waals interaction, and columbic electrostatic potentials. The potential energy of the initial structure was minimized using the method of Conjugate Gradient (Fletcher−Reeves).

Fluorescence Photopatterning. Photo-cross-linkings of the polymer films were conducted using a 365 nm UV light at ∼30 mW/cm^2 as the irradiation source. A 1,2-dichloroethane solution of *hb*-PSP(6) (sample taken from Table 2, no. 15) was prepared in a concentration of ∼2 wt %. A thin solid film was fabricated by spin-coating the solution at 2000 rpm for 1 min on a silicon wafer. The polymer film was dried in a vacuum oven at room temperature overnight, which was then covered by a Cu-negative mask and irradiated by the UV light. Afterward, the silicon wafer was dipped into 1,2-dichloroethane for 40 s to remove the un-cross-linked parts from the wafer. The resulting pattern was dried in a vacuum oven at room temperature overnight. Fluorescent image of the photopattern was taken under a fluorescence optical microscope (Olympus BX41) with 330−385 nm wide bands of UV excitation.

Acknowledgment. This work was partly supported by the Research Grants Council of Hong Kong (602706, HKU2/05C, 603505, and 603304), the National Science Foundation of China (20634020), and the Ministry of Science & Technology of China (2002CB613401). B.Z.T. expresses thanks for the support from the Cao Guangbiao Foundation of Zhejiang University.

Supporting Information Available: Text giving explanations for ideal growth pattern, mathematical deductions for eqs 22 and 23, and detailed modeling strategy elaboration, a chart showing the structures used, tables of mathematical relationships and potential energies, a scheme showing the structural changes, and a figure showing TGA thermograms of the *hb*-PSPs taken in air. This material is available free of charge via the Internet at http://pubs.acs.org.

References and Notes

(1) Thompson, D. S.; Markoski, L. J.; Moore, J. S.; Sendijarevic, I.; Lee, A.; McHugh, A. J. *Macromolecules* **2000**, *33*, 6412.
(2) Sunder, A.; Hanselmann, R.; Frey, H.; Mulhaupt, R. *Macromolecules* **1999**, *32*, 4240.
(3) Chang, H. T.; Fréchet, J. M. J. *J. Am. Chem. Soc.* **1999**, *121*, 2313.
(4) Xu, M. H.; Zhang, H. C.; Pu, L. *Macromolecules* **2003**, *36*, 2689.
(5) Hao, J.; Jikei, M.; Kakimoto, M. *Macromolecules* **2003**, *36*, 3519.
(6) Voit, B. *J. Polym. Sci., Polym. Chem.* **2000**, *38*, 2505.
(7) Inoue, K. *Prog. Polym. Sci.* **2000**, *25*, 453.
(8) Hawker, C. J. *Curr. Opin. Colloid Interface Sci.* **1999**, *4*, 117.
(9) Zhi, L.; Wu, J.; Li, J.; Stepputat, M.; Kolb, U.; Mullen, K. *Adv. Mater.* **2005**, *17*, 1492.
(10) Wooley, K. J.; Hawker, C. J.; Lee, R.; Frechet, J. M. J. *Polym. J.* **1994**, *26*, 187.
(11) Corriu, Robert, J. P. *Angew. Chem., Int. Ed.* **2000**, *39*, 1376.
(12) Kwak, G.; Fujiki, M.; Masuda, T. *Macromolecules*, **2004**, *37*, 2422.
(13) Yoon, K.; Son, D. Y. *Macromolecules* **1999**, *32*, 5210.
(14) Oishi, M.; Minakawa, M.; Imae, I.; Kawakami, Y. *Macromolecules* **2002**, *35*, 4938.
(15) Zheng, R.; Dong, H.; Tang, B. Z. In *Macromolecules Containing Metal- and Metal-Like Elements*; Abd-El-Aziz, A., Carraher, C., Pittman, C., Sheats, J., Zeldin, M., Eds.; Wiley: New York, 2005; Vol. 4, Chapter 2, p 7.
(16) Sun, Q.; Xu, K.; Peng, H.; Zheng, R.; Häussler, M.; Tang, B. Z. *Macromolecules* **2003**, *36*, 2309.
(17) Kwak, G.; Masuda, T. *Macromol. Rapid Commun.* **2002**, *23*, 68.
(18) Rao, T. V.; Yamashita, H.; Uchimaru, Y.; Sugiyama, J.; Takeuchi, K. *Polymer*, **2005**, *46*, 9736.
(19) Kwak, G.; Takagi, A.; Fujiki, M.; Masuda, T. *Chem. Mater.* **2004**, *16*, 781.
(20) Tang, B. Z.; Xu, K.; Sun, Q.; Lee, P. P. S.; Peng, H.; Salhi, F.; Dong, Y. *ACS Symp. Ser.* **2000**, *760*, 146.
(21) Lam, J. W. Y.; Luo, J.; Peng, H.; Xie, Z.; Xu, K.; Dong, Y.; Cheng, L.; Qiu, C.; Kwork, H. S.; Tang, B. Z. *Chin. J. Polym. Sci.* **2001**, *19*, 585.
(22) Häussler, M.; Lam, J. W. Y.; Zheng, Y.; Peng, H.; Luo, J.; Chen, J.; Law, C. C. W.; Tang, B. Z. *C. R. Chim.* **2003**, *196*, 289.
(23) Lam, J. W. Y.; Chen, J.; Law, C. C. W.; Peng, H.; Xie, Z.; Cheuk, K. K. L.; Kwork, H. S.; Tang, B. Z. *Macromol. Symp.* **2003**, *196*, 289.
(24) Häussler, M.; Dong, H. C.; Lam, J. W. Y.; Zheng, R.; Qin, A.; Tang, B. Z. *Chin. J. Polym. Sci.* **2005**, *23*, 567.
(25) Häussler, M.; Tang, B. Z. *Adv. Polym. Sci.* **2007**, *209*, 1.
(26) Xu, K.; Tang, B. Z. *Chin. J. Polym. Sci.* **1999**, *17*, 397.
(27) Peng, H.; Luo, J.; Cheng, L.; Lam, J. W. Y.; Xu, K.; Dong, Y.; Zhang, D.; Huang, Y.; Xu, Z.; Tang, B. Z. *Opt. Mater.* **2002**, *21*, 315.
(28) Xu, K.; Peng, H.; Sun, Q.; Dong, Y.; Salhi, F.; Luo, J.; Chen, J.; Huang, Y.; Zhang, D.; Xu, Z.; Tang, B. Z. *Macromolecules* **2002**, *35*, 5821.
(29) Peng, H.; Cheng, L.; Luo, J.; Xu, K.; Sun, Q.; Dong, Y.; Salhi, F.; Lee, P. P. S.; Chen, J.; Tang, B. Z. *Macromolecules* **2002**, *35*, 5349.
(30) Chen, J.; Peng, H.; Law, C. C. W.; Dong, Y.; Lam, J. W. Y.; Williams, I. D.; Tang, B. Z. *Macromolecules* **2003**, *36*, 4319.
(31) Zheng, R.; Lam, J. W. Y.; Peng, H.; Häussler, M.; Tang, B. Z. *Polym. Mater. Sci. Eng.* **2003**, *88*, 365.
(32) Häussler, M.; Liu, J. Z.; Zheng, R.; Tang, B. Z. *Macromolecules* **2007**, *40*, 1914.
(33) Lam, J. W. Y.; Tang, B. Z. *Acc. Chem. Res.* **2005**, *38*, 745.
(34) Eaborn, C.; Jones, K. L.; Lickiss, P. D. *J. Organomet. Chem.* **1993**, *461*, 31.
(35) Bott, R.; Eaborn, W. C.; Jackson, P. M. *J. Organomet. Chem.* **1967**, *7*, 79.
(36) Eaborn, C. *J. Organomet. Chem.* **1975**, *100*, 43.
(37) *Materials Studio*; Accelrys software.
(38) Luo, J.; Xie, Z.; Lam, J. W. Y.; Cheng, L.; Chen, H.; Qiu, C.; Kwok, H. S.; Zhan, X.; Liu, Y.; Zhu, D.; Tang, B. Z. *Chem. Commun.* **2001**, 1740.

MA071062D